Materials Today Bio 28 (2024) 101231

Contents lists available at ScienceDirect

Materials Today Bio

journal homepage: www.journals.elsevier.com/materials-today-bio

Calcium enrichment activity initiates extracellular calcium influx-dependent inflammatory response of biologically-derived hydroxyapatite

Chuangji Li [a,b,c,1], Mengxi Su [a,b,c,1], Meihua Mai [a,b,c,1], Zefeng Guo [a,b,c], Ye Li [a,b,c], Shoucheng Chen [a,b,c], Quan Liu [a,b,c], Danying Chen [a,b,c], Xiayi Wu [a,b,c], Zetao Chen [a,b,c,*], Zhuofan Chen [a,b,c,**], Shiyu Wu [a,b,c,***]

[a] Hospital of Stomatology, Sun Yat-sen University, Guangzhou, 510055, China
[b] Guanghua School of Stomatology, Sun Yat-sen University, Guangzhou, 510055, China
[c] Guangdong Provincial Key Laboratory of Stomatology, Guangzhou, 510055, China

ARTICLE INFO

Keywords:
Hydroxyapatite
Calcium enrichment
Calcium influx
Inflammatory response
Macrophage

ABSTRACT

Biologically-derived hydroxyapatite is a widely used biomaterial in various clinical applications including bone augmentation. However, the osteogenic application of biological hydroxyapatite is limited by inflammatory responses, and the underlying mechanism remains unknown. The current study aimed to elucidate the molecular mechanisms underlying the inflammatory response to biological hydroxyapatite. Porcine-derived hydroxyapatite (PHA) with two sintering temperatures (800 and 1600 °C), PHA800 and PHA1600, respectively, were prepared. A PHA/macrophage co-culture model was established. Transcriptome, polymerase chain reaction (PCR), and enzyme-linked immunosorbent assay (ELISA) analyses were used to determine the inflammatory effects and the main pathways activated by PHA800 and PHA1600. Intracellular calcium level, PHA-induced calcium enrichment, and related biological effects were used to determine the molecular mechanism at the PHA-cell interface. PHA800 significantly upregulated a TLR4 mediated inflammatory pathway in a calcium influx-dependent manner, and the calcium enrichment activity on the surface of PHA800 promoted calcium influx. In contrast, the calcium enrichment activity on the surfaces of the PHA1600 and PHA800 pretreated groups was attenuated, resulting in decreased calcium influx and mild inflammatory effects. Our results provide a fundamental basis for the development of novel bone substitutes that elicit low levels of inflammation response.

1. Introduction

Hydroxyapatite bone substitutes have been widely used in bone regeneration. Compared to autologous bone, bone substitutes eliminate the need for a second surgery site, which significantly reduces pain in patients. Therefore, bone substitutes are ideal bone augmentation strategy. However, the simple application of bone substitutes has some limitations, including long clinical treatment cycles and limited bone formation [1,2]. Therefore, the development of novel bone substitutes with high osteogenic efficiency is of significant clinical value.

The proinflammatory effect of hydroxyapaptite both *in vitro* and *in vivo* has garnered significant attention [3,4]. Clinically, patients implanted with bone substitutes are more prone to swelling in the early stages, suggesting the occurrence of inflammatory reaction. According to the osteoimmunomodulation theory, excessive inflammatory reactions triggered by biomaterials are not conducive to long-term regeneration [5–7]. This is consistent with the findings of clinical and basic studies on hydroxyapatite bone substitutes. Clinical studies indicate that the utilization of bone substitutes alone results in a notable prolongation of the healing time for bone regeneration, extending it by

* Corresponding author. Hospital of Stomatology, Sun Yat-sen University, Guangzhou, 510055, China.
** Corresponding author. Hospital of Stomatology, Sun Yat-sen University, Guangzhou, 510055, China.
*** Corresponding author. Hospital of Stomatology, Sun Yat-sen University, Guangzhou, 510055, China.
E-mail addresses: chenzet3@mail.sysu.edu.cn (Z. Chen), chzhuof@mail.sysu.edu.cn (Z. Chen), wushy55@mail.sysu.edu.cn (S. Wu).
[1] These authors contributed equally.

https://doi.org/10.1016/j.mtbio.2024.101231
Received 10 May 2024; Received in revised form 10 August 2024; Accepted 3 September 2024
Available online 4 September 2024

3–6 months in comparison with the use of autogenous bone or a combination of the two [1]. Moreover, basic research has revealed that the initial bone healing process is delayed when bone substitutes are used [8] compared to the natural healing process. These evidence indicate that hydroxyapatite-induced inflammation may impede the initiation of the bone regenerative process [5], which would suppress the osteogenic efficacy and result in delay of bone healing process [8,9]. Therefore, clarifying the inflammatory mechanism of hydroxyapatite bone substitutes is of great significance for the development of novel low-inflammatory bone substitutes with improved osteogenic efficacy.

Among the various bone substitutes, biologically-derived hydroxyapatite (BHA) especially from mammalian bones (e.g., bovine, camel, equine, and porcine) is widely used in clinical practice and laboratory studies. Heat treatment is an important step during BHA preparation that is used to eliminate organic components and prevent the risk of immunological reactions and disease transmission [10]. The sintering temperature exhibits a strong correlation with the hydroxyapatite-induced inflammatory response, potentially because of alterations in the morphology and microstructure caused by the sintering process [4,11,12]. The underlying mechanism may be related to the activation of TLR4 receptors [13]. However, the specific inflammatory mechanisms of BHA require further investigation.

In this study, we analyzed porcine bone-derived hydroxyapatite (PHA) prepared at two different sintering temperatures (800 °C and 1600 °C). After establishing a direct co-culture model, transcriptomics was used to identify the immune-regulatory effects and main activated pathways. The molecular mechanisms in the PHA-cell interface was then elucidated. The aim of the study was to elucidate the inflammatory mechanisms of PHA. These results would provide optimized targets for the development of novel low-inflammatory biologically-derived bone substitutes.

2. Results and discussion

2.1. Establishment of in vitro direct co-culture model

Previous studies have shown that macrophage (MΦ) is one of the immune cells with unique regulatory ability and excellent plasticity when interacting with biomaterials. Therefore, we focused on macrophage to investigate how the bone substitute regulates their inflammatory responses. The core requirement of an *in vitro* model is that it recapitulate the complex interactions between the materials and cells. Based on previous studies [14–17], PHA was prepared and sintered at two different temperatures (800 °C and 1600 °C) to generate PHA800 and PHA1600 (Fig. 1A). PHA1600 exhibited increased grain size, aggregation tendency, crystallinity, with similar elemental distribution compared to PHA800 (Fig. 1BC).

The appropriate form of material-cell contact that reflects the cellular inflammatory response was then explored. First, an indirect culture model was established (Fig. 2A). The model showed optimal cell viability (Fig. 2, a1), and allowed for effient isolation of RNA (Fig. 2, a2). However, PCR revealed very mild inflammatory reaction in the cells (Fig. 2, a3), indicating that the indirect culture model may not accurately evaluate the inflammatory response to hydroxyapatite. Next, a co-culture model was established. Conventional sized apatite particles were used for co-culture in strategy 2 (Fig. 2B). Results of the CCK-8 assay showed that cell viability was not significantly affected (Fig. 2, b2), but RNA could not be effectively extracted (Fig. 2, b3), indicating high affinity for nucleic acids of hydroxyapatite that could separate DNA/RNA from other cellular components [18]. Therefore, the co-culture model was modified, and fine-grained apatite was used in strategy 3 (Fig. 2C). The CCK-8 assay revealed that cell viability was unaffected in this model (Fig. 2, c2, Supplementary Fig. 1). In terms of RNA extraction, although RNA could not be effectively extracted in the 5 mg/mL PHA group, it could be effectively extracted in the 0.04, 0.2, and 1 mg/mL PHA groups (Fig. 2, c3, Supplementary Fig. 1). PCR was performed in the 0.2 and 1 mg/mL groups to evaluate cellular inflammatory effects. The 1 mg/mL group effectively reflected the cellular inflammatory effects (Fig. 2, c4). Therefore, a 1 mg/mL concentration of the material was used for the *in vitro* co-culture models in subsequent experiments.

It should be noted that RNA extraction from cells co-cultured with clinically-used conventional-sized hydroxyapatite has always been a challenge because of the adsorption of hydroxyapatite [19]. To resolve this problem, it is necessary to modify the material, use alternative

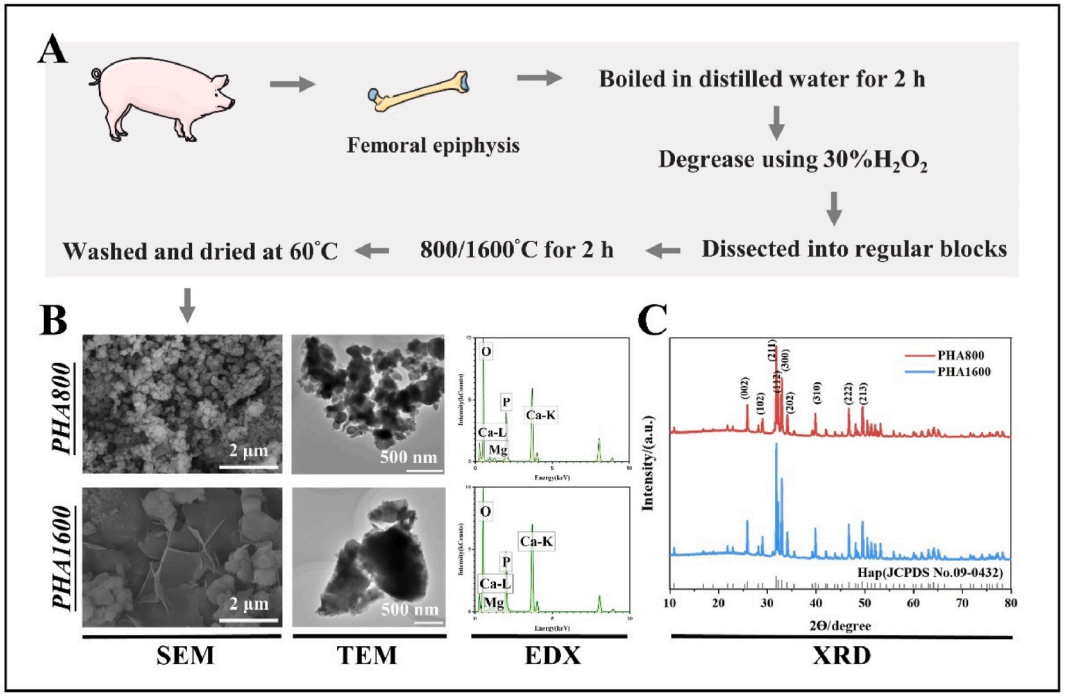

Fig. 1. Preparation and characterization of porcine bone-derived hydroxyapatite (PHA). (A) Preparation flow diagram. (B) Morphological and elemental distribution detection via SEM, TEM and EDX. (C) XRD detection.

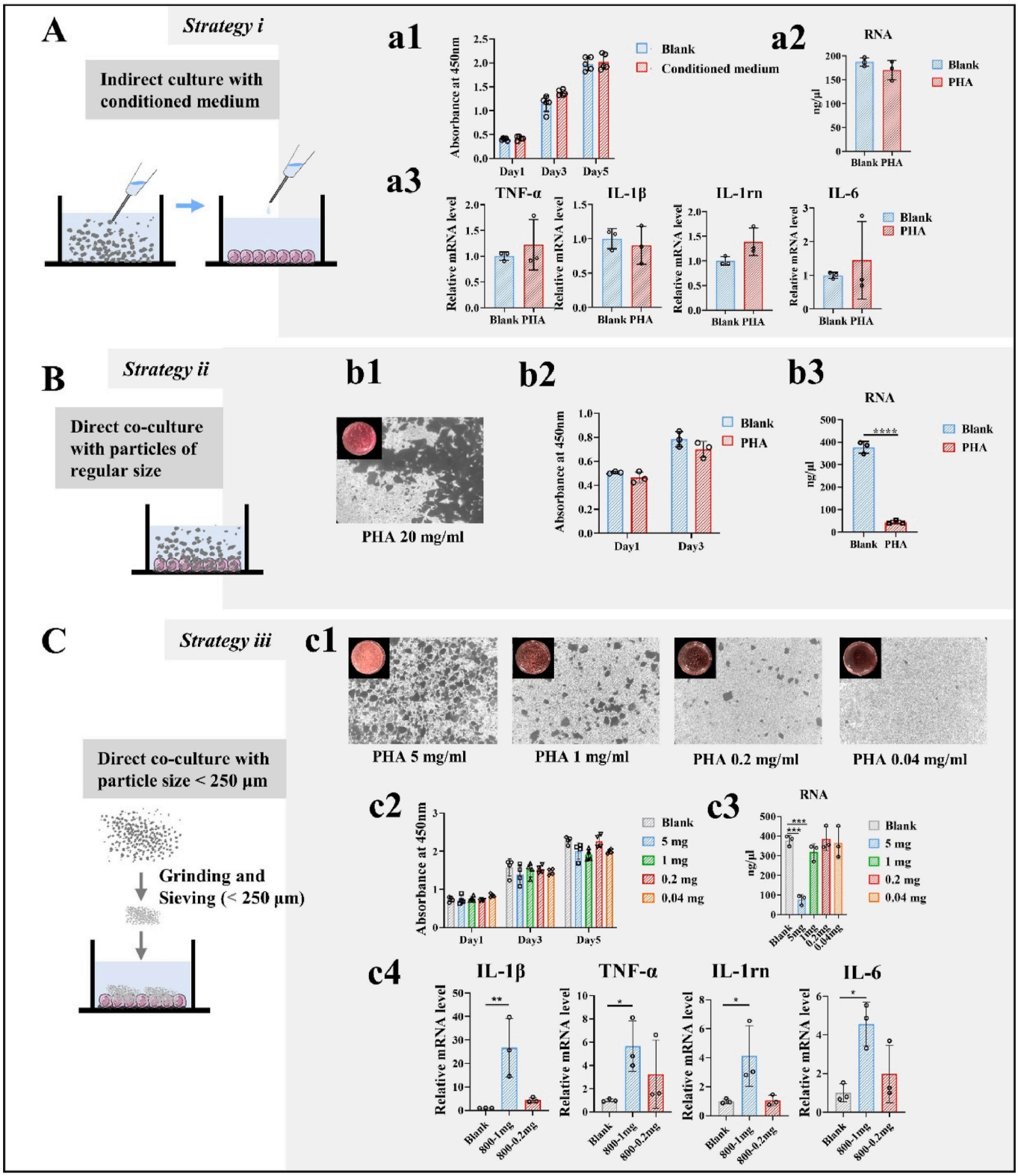

Fig. 2. Establishment of co-culture model *in vitro*. (A) Strategy i: Indirect culture with conditioned medium. (B) Strategy ii: Direct culture with particles of regular size. (C) Strategy iii: Direct culture with particle size below 250 μm. (a1, b2, c2) CCK-8 cytotoxicity test (n = 5). (b1, c1) Optical microscopy observation. (a2, b3, c3) RNA quantitative detection (n = 3). (a3, c4) Canonical inflammatory genes expression of macrophages (n = 3). The data are expressed as means ± standard deviation (SD). Statistical analysis was conducted using the unpaired two-tailed Student's t-test and ANOVA, followed by Tukey's multiple comparison post hoc test. $^{*}p < 0.05$, $^{**}p < 0.01$, $^{***}p < 0.001$, and $^{****}p < 0.0001$.

detection methods, such as immunofluorescence and ELISA, or switch to an indirect culture model. In the present study, we refer to the cell co-culture method of nano hydroxyapatite [20–22]. Due to methodological constraints, this study focused on the immunological properties of bone substitute materials with particle sizes less than 0.25 mm. Further research is needed to explore the immunological properties of bone substitute with particle sizes greater than 0.25 mm.

2.2. PHA800 induced a TLR4-mediated inflammatory response in an extracellular calcium influx-dependent manner

It is well documented that hydroxyapatite induces inflammation by

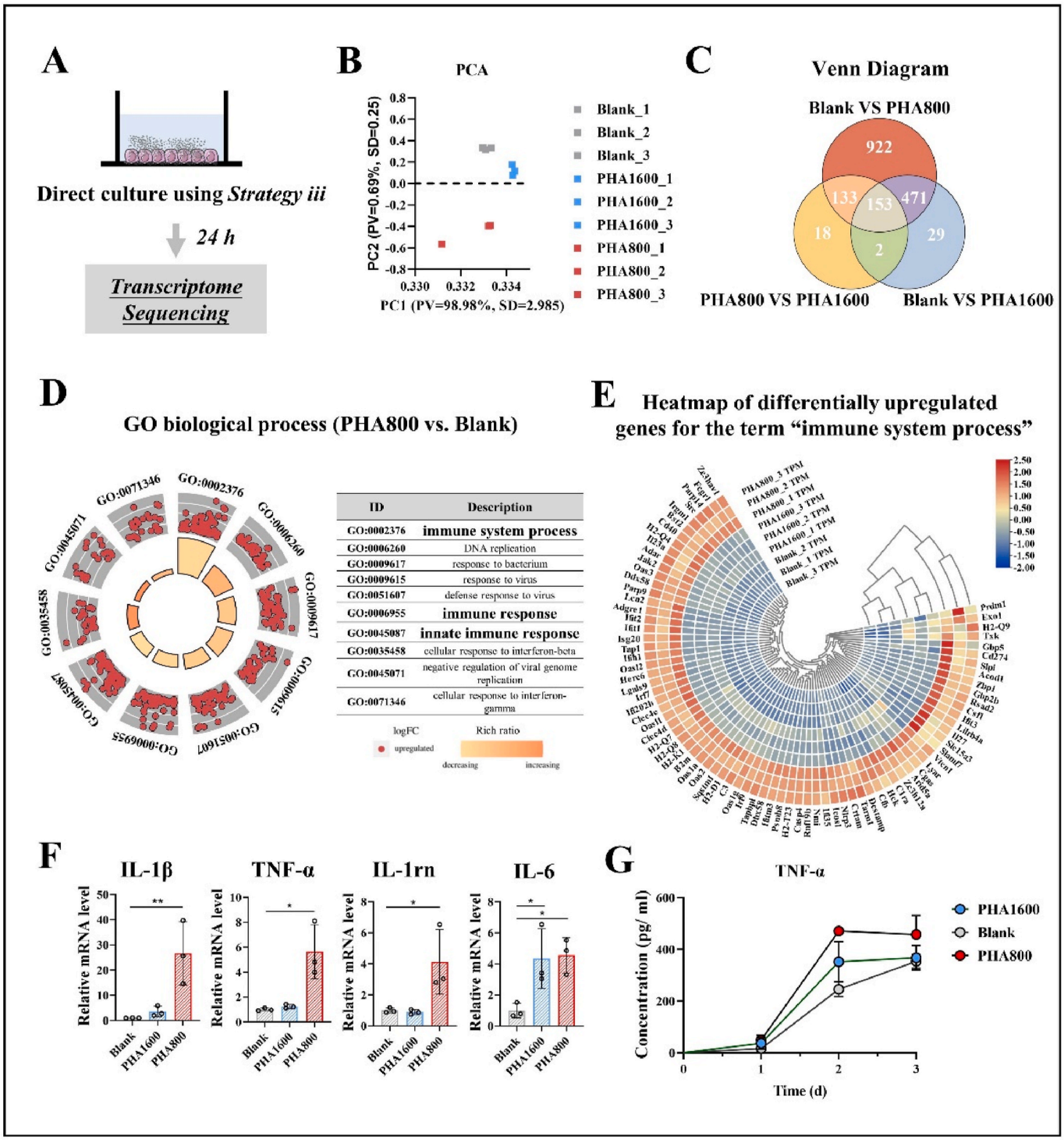

Fig. 3. PHA800 triggered significant inflammatory response of macrophages. (A) Schematic diagram of co-culture using strategy iii for 24 h followed by transcriptome sequencing. (B) The principal component analysis (PCA). (C) Venn diagram. (D) The top 10 terms of GO analysis for biological process in differentially upregulated genes (PHA800 vs. Blank). (E) Heatmap of differentially upregulated genes for immune system-related terms. (F–G) RT-qPCR (F) and ELISA (G) of canonical inflammatory gene/protein expression of macrophages. Different expressed RNAs with |log2(FC)| value > 1 and adjusted p-value <0.05 were deemed significant for further analysis. Statistical analysis was conducted using the ANOVA followed by Tukey's multiple comparison post hoc test. *$p < 0.05$, **$p < 0.01$, ***$p < 0.001$, and ****$p < 0.0001$.

activating the TLR4 pathway. Because PHA shares a similar chemical composition and structure with hydroxyapatite, we hypothesized that PHA may trigger inflammation by activating the TLR4 pathway. To test this hypothesis, we used transcriptomics, PCR, and ELISA to analyze specific pathways. Principal component analysis (PCA) showed good quality control of the transcriptome samples (Fig. 3B). Total gene expression variations were determined using a Venn diagram (Fig. 3C), volcano plots, and a cluster heatmap of gene expression (Supplementary Fig. 2). The cluster heatmap showed that blank vs. PHA800 had the largest number of differential genes, whereas blank vs. PHA1600 had more similar gene expression patterns than blank vs. PHA800. Gene ontology (GO) enrichment analysis revealed upregulation of immune-related terms in the PHA800 group compared with that in the blank group (Fig. 3D–Supplementary Table 1). The cluster heatmap from the immune system-related terms demonstrated significant upregulation of inflammation-related genes in the PHA800 group, whereas the PHA1600 and blank groups shared similar expression levels of immune-related genes (Fig. 3E). PCR and ELISA verified the gene and protein expression levels of the canonical inflammatory factors (*IL-1β, IL-1Rn, TNF-α, and IL-6*) (Fig. 3F and G).

To identify the specific activated pathways, GO enrichment analysis was performed between PHA800 and PHA1600, highlighting immune system process and external side of the palsma membrane as predominant terms (Fig. 4A and B, and Supplementary Tables 2 and 3). Kyoto Encyclopedia of Genes and Genomes (KEGG) revealed the top five enriched pathways, highlighting multiple inflammatory pathways including NOD-like receptor and NF-κB signaling pathways (Fig. 4C–Supplementary Table 4). The gene heatmap related to the NOD-like receptor signaling pathway showed an obvious increase in the PHA800 group compared to that in the PHA1600 and blank groups (Fig. 4D). Reactome enrichment analysis was then used, highlighting a differentially upregulated signaling pathway of the TLR4 cascade based on genes in NOD-like receptor and NF-κB signaling pathways (Fig. 4E). The gene heatmap related to the Toll-like receptor signaling pathway showed an obvious increase in the PHA800 group compared to that in the PHA1600 and blank groups (Fig. 4F). The upregulation of TLR4-MyD88-independent pathway was noticed which was in accordance with previous study using nano hydroxyapatite [23] (Fig. 4E). The TLR4 activation may further activate the NOD pathway and the downstream pathways, including NF-κB (Fig. 4CD), due to the crosstalk between TLR4-and NOD1/2 [24]. Therefore, the biologically-derived bone substitutes may activate a variety of canonical inflammatory pathways, such as MyD88-independent, NOD, and NF-κB pathways through TLR4 activation. The upregulation of the key genes in the TLR4-and NOD-related signaling pathway were then verified (Fig. 4G).

Research with LPS model has confirmed that TLR4 recognizes the surface structure of LPS, when the extracellular calcium influx through calcium channels such as TRPM7 assisted [25]. Based on this, we hypothesized that calcium influx is required for PHA-induced TLR4 activation of macrophage. Calcium influx was first confirmed in the PHA800 group (Fig. 5A–C). The intracellular Ca^{2+} concentration in macrophages significantly increased between 12 and 24 h in the PHA800 group compared to that in PHA1600 and blank groups (Fig. 5BC). A specific TRPM7 calcium channel blocker, FTY720, was used to establish a calcium blockade model (Fig. 5D). Following FTY720 treatment, the intracellular Ca^{2+} concentration was significantly lower than that of the blank group (Fig. 5E), suggesting that the calcium blockade model was successfully established. PCR verified that most of the canonical inflammatory factors were significantly downregulated or showed no significant difference compared with that in the blank group (*TNF-α, IL-1rn, IL-6, IL-1β, NF-κB, NLRP3*) (Fig. 5F), which strongly supports the hypothesis.

Previous studies on nano-HA have hypothesized that TLR activation requires calcium influx for auxiliary activation [20]. To the best of our knowledge, this is the first study to confirm that the xenograft PHA activates macrophage TLR4-mediated inflammatory pathway in an extracellular calcium influx-dependent manner. Patricia et al. identified a similar mechanism in a study of the BCP/blood cell complex [9]. This complex induces inflammation by activating TLR- and NOD-axes peripheral blood mononuclear cells. The authors proposed that the activation of the NOD axis was mainly due to BCP-induced calcium-deficient hemolysis, followed by an increase in extracellular ATP. As blood and blood cell components were not involved in the current *in vitro* model, we believe that the inflammation mainly originates from the direct stimulation of the xenografts.

2.3. Calcium enrichment activity at the PHA800 surface induces extracellular calcium influx

After confirming calcium influx, extracellular calcium sources were futher investigated. Xenograft materials can enrich the culture medium with calcium ions, as reported previously [26]. The calcium ion enrichment properties of PHA800 and PHA1600 were determined using ICP. The results showed that after 24 h of immersion, PHA800 enriched calcium ions in the culture medium, whereas PHA1600 did not (Fig. 6A). These evidence arose hypothesis that the enrichment of Ca^{2+} on the surface of PHA800 triggers calcium influx and subsequent biological effects, whereas the PHA1600 interface did not adsorb Ca^{2+} and failed to initiate subsequent calcium influx or inflammatory effects.

As the different morphology of PHA800 and PHA1600 may affect immune response (Fig. 1), the hypothesis that calcium enrichment may trigger calcium influx cannot be fully confirmed by the above tests. We set PHA800 and PHA800-pretreated groups with the same morphology, composition and structure. Using sequential ICP detection, calcium ion enrichment activity was observed over time (Fig. 6B). The enrichment activity was the strongest in the first 30 min and gradually weakened to reach a plateau at approximately 48 h, indicating that the calcium enrichment activity ended after infiltrating the culture medium for 48 h. The PHA800 group pretreated with Dulbecco's modified Eagle's medium (DMEM) for 48 h was designated as PHA800-pretreated group, abbreviated PHA800 (pre) (Fig. 6C). Such setting can further demonstrate the role of calcium enrichment activity in activating inflammation.

Analysis of intracellular Ca^{2+} levels confirmed that the degree of calcium influx in PHA800 (pre) was significantly lower than that in PHA800 at the end of the calcium enrichment activity (Fig. 6D), indicating that calcium enrichment activity enhances calcium influx. PCR and ELISA revealed that the expression of inflammatory factors in PHA800 (pre) group was significantly lower than that in the PHA800 group (Fig. 6E and F), confirming that calcium enrichment activity directly participates in the regulation of inflammation through calcium influx. Transmission electron microscopy (TEM) analysis revealed that no significant change in the micromorphology of the two groups. Unlike in a previous study [27], no rod-like crystals were observed (Fig. 6G), which ruled out the potential influence of morphological differences. X-ray diffraction (XRD) confirmed that the crystallinity of PHA800 (pre) was lower than that of PHA800 (Fig. 6H), indicating that the calcium enrichment activity is caused by calcium phosphorus crystallization process at the PHA800 interface rather than a transient adsorption process. The specific crystallization mechanism may involve potential adsorption, which requires further research.

2.4. Implications for the development of novel low-inflammatory bone substitute

The process of osteogenesis induced by bone repair materials is multifaceted, involving factors such as surgical technique, the morphology of the remaining bone, and immune reactions. Although PHA1600 showed mitigated inflammation, its osteogenic capacity tends to diminish as the pore structure is compromised when the temperature exceeds 1000 °C [28–30], since high-temperature (>1000 °C) sintered materials may not be conducive for the growth of cells and bone

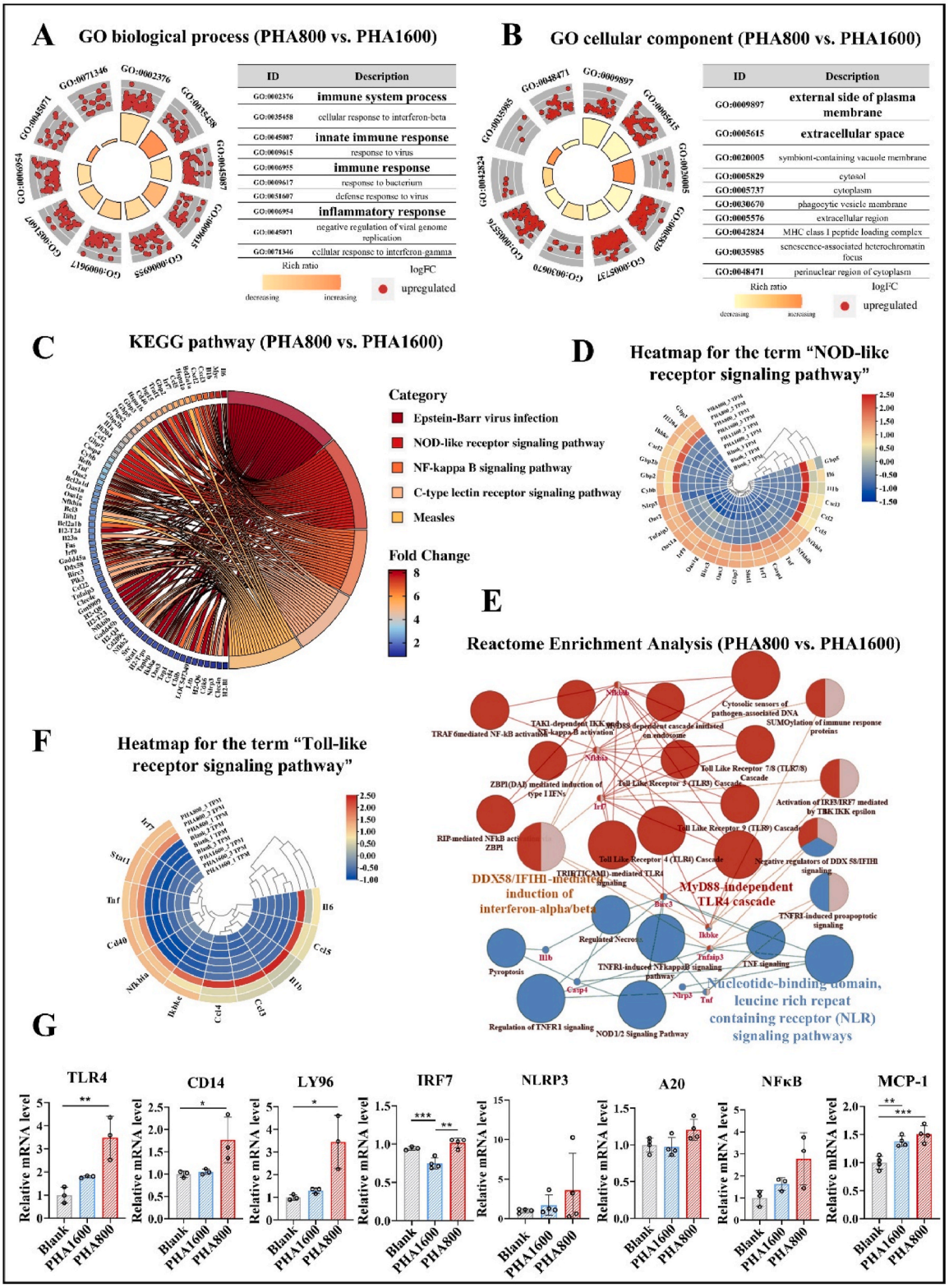

Fig. 4. PHA800 induced inflammatory response of macrophages via a potential TLR4- and NOD-related pathways. (A–B) The GO enrichment analysis shows the top 10 terms for biological process (A) and cellular component (B) in differentially upregulated genes (PHA800 vs. PHA1600). (C) KEGG analysis reveals the top 5 pathways enriched in differentially upregulated genes (PHA800 vs. PHA1600). (D) Heatmap of differentially upregulated genes for the term "NOD-like receptor signaling pathway". (E) The Reactome enrichment analysis highlighting a differentially upregulated signaling pathway of TLR4 cascade based on genes in NOD-like receptor signaling pathway and the NF-κB signaling pathway (PHA800 vs. PHA1600) by ClueGO. (F) Heatmap of differentially upregulated genes for the term "Toll-like receptor signaling pathway". (G) RT-qPCR of canonical gene expression related to the TLR4- and NOD-signaling pathways in macrophages. Different expressed RNAs with |log2(FC)| value > 1 and adjusted p-value <0.05 were deemed significant for further analysis. Statistical analysis was conducted using the ANOVA followed by Tukey's multiple comparison post hoc test. *$p < 0.05$, **$p < 0.01$, ***$p < 0.001$, and ****$p < 0.0001$.

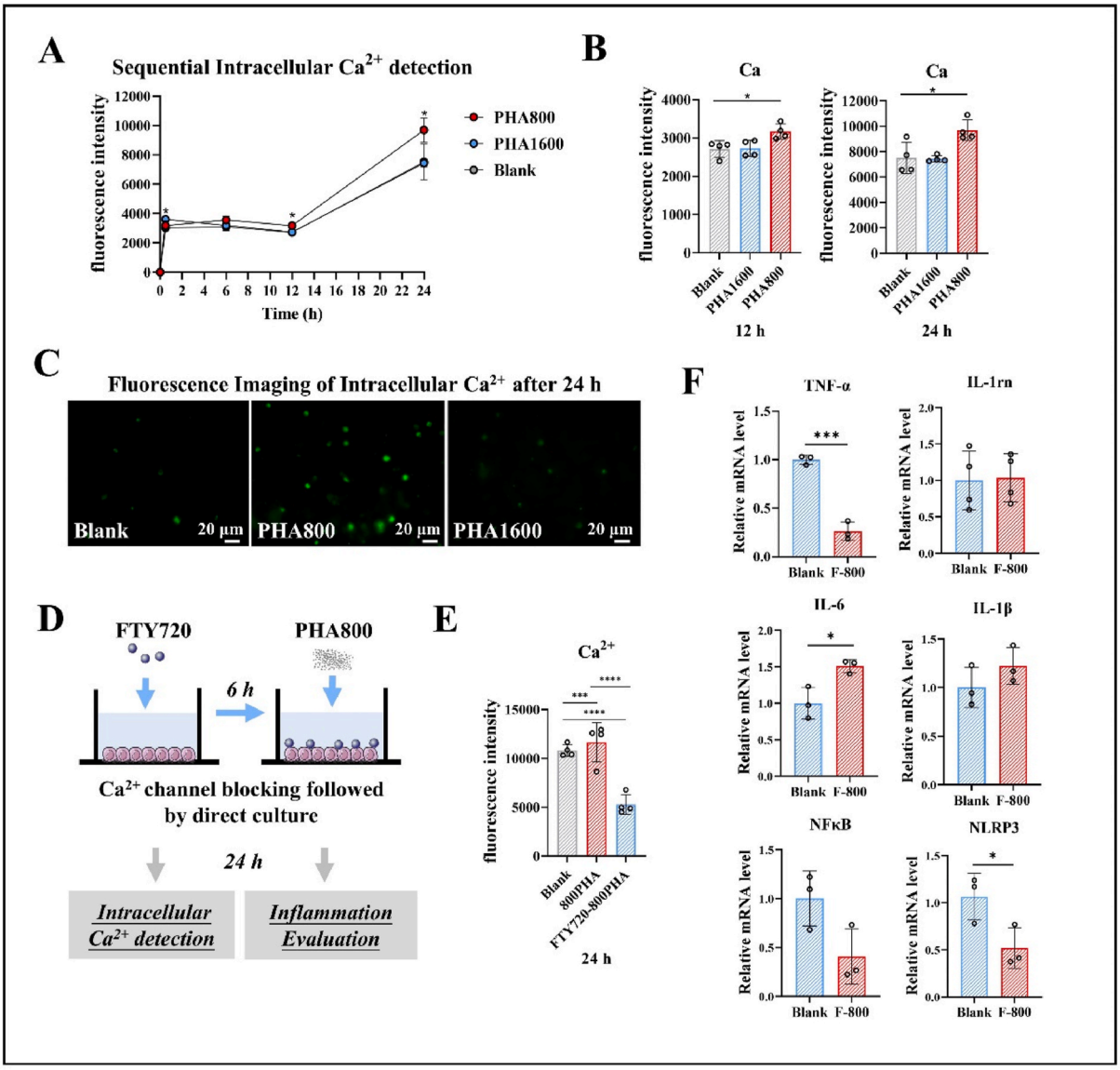

Fig. 5. Calcium influx is essential for PHA800-induced inflammation. (A) Sequential intracellular Ca^{2+} detection from 30 min to 24 h using fluorescence intensity. (B) Intracellular Ca^{2+} level at 12 h and 24 h. (C) Fluorescence imaging of intracellular Ca^{2+} after 24 h stimulation. (D) Schematic diagram of the establishment of calcium channel blockade model. (E) Intracellular Ca^{2+} detection after FTY720 treated. (F) RT-qPCR of canonical inflammatory gene expression after treated with FTY720. Statistical analysis was conducted using the unpaired two-tailed Student's t-test and ANOVA, followed by Tukey's multiple comparison post hoc test. $*p < 0.05$, $**p < 0.01$, $***p < 0.001$, and $****p < 0.0001$.

formation [31]. As for PHA800, bone regeneration is still possible once the inflammatory phase subsides. This is attributed to the use of a barrier membrane in clinical practice, which confines the inflammatory environment to the bone microenvironment to some extent. We hypothesize that if the inflammatory response triggered by PHA800 were mitigated, its osteogenic efficiency could be further enhanced. Consequently, the findings of this study do not endorse the idea that high-temperature sintered materials inherently surpass those sintered at lower temperatures. The results are intended solely to elucidate the impact of sintering temperature on the inflammatory response of macrophages.

Based on the results of the present study, we propose the following strategies to alleviate the proinflammatory effects of hydroxyapatite: **Calcium enrichment activity induced *in vitro*:** As PHA800 (pre) showed a decrease in the level of inflammation, pretreatment with calcium- and phosphorus-containing solutions *in vitro* (e.g., culture medium, blood, and serum) to reduce the active level of surface calcium enrichment may effectively reduce the inflammatory response of hydroxyapatite. Specific procedures for clinical applications, such as solvent type and pretreatment duration, will be determined in subsequent studies. **Organic coating:** Bone substitutes with organic-coating, such as gelatin, collagen, chitosan, and hyaluronic acid, have been widely developed in clinics and laboratories. From the perspective of hydroxyapatite, organic coating can reduce the degree of hydroxyapatite contact with immune cells in the early stage. Ideally, hydroxyapatite should undergo calcium enrichment in the humoral environment until a stable crystal phase is reached. Immune cells preferentially recognize organic components, and this will help to avoid the inflammatory effect of immune cells triggered by calcium enrichment activity, so as to create an improved microenvironment for bone regeneration. **Nutrient trace element modification:** Hydroxyapatite has abundant active binding sites, which can be used to introduce inorganic ions (e.g., fluorine, zinc, magnesium, and copper) to regulate the immune microenvironment and improve the osteogenic efficiency of osteoblasts [32–35]. The mixed use of these strategies may have better synergistic effects, which requires further research.

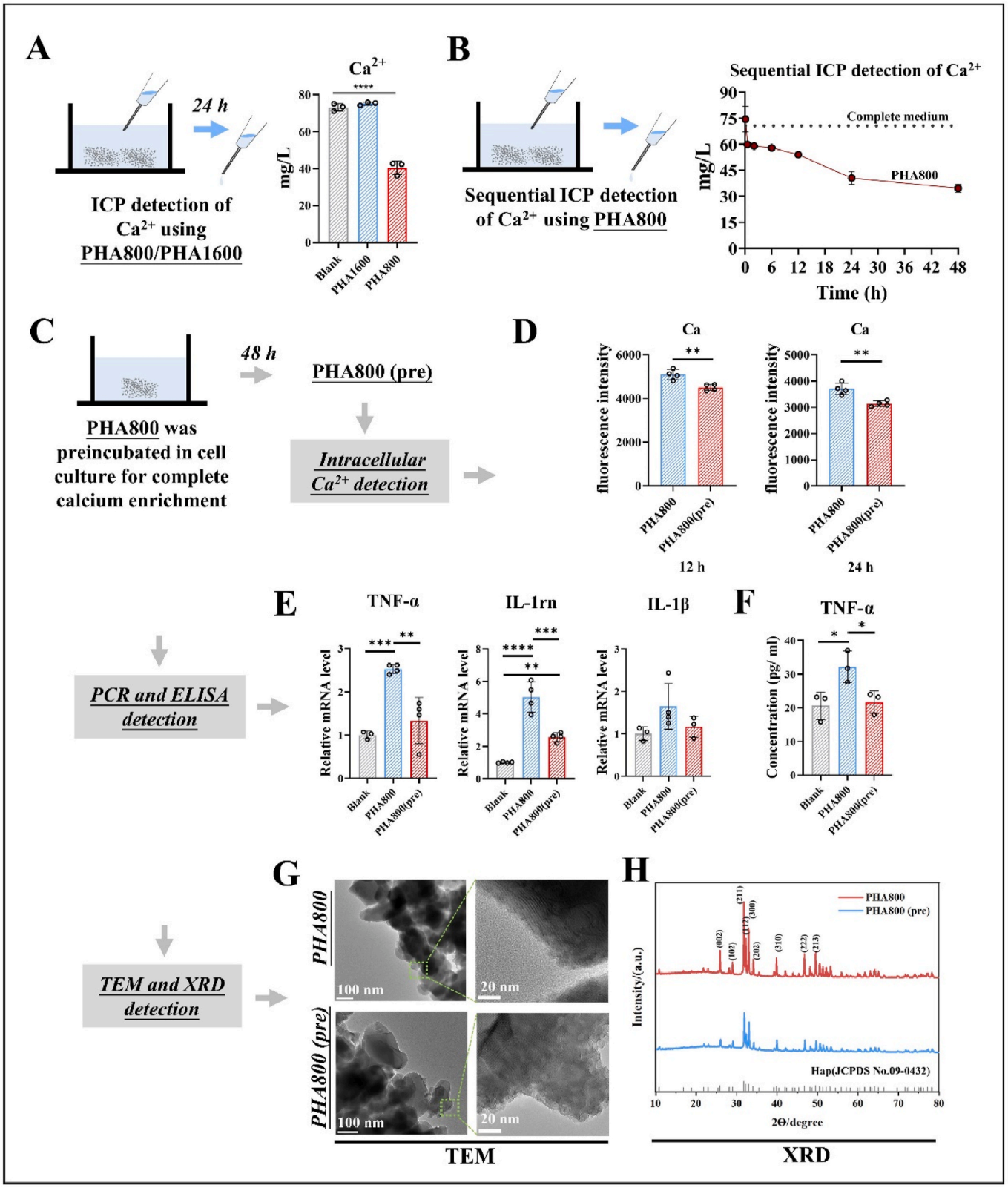

Fig. 6. Calcium enrichment activity induced calcium influx-related inflammatory response. (A) ICP detection of Ca^{2+} in supernatant of PHA800 and PHA1600. (B) Sequential ICP detection of Ca^{2+} in supernatant of PHA800 from 5 min to 48 h. (C) Schematic diagram of the preparation of PHA800 pretreatment. (D) Intracellular Ca^{2+} level of PHA800 and PHA800 (pre) at 12 h and 24 h. (E–F) RT-qPCR (E) and ELISA (F) of canonical inflammatory gene/protein expression of macrophages in PHA800 and PHA800 (pre). (G) TEM observation of PHA800 and PHA800 (pre). (H) XRD detection of PHA1600, PHA800 and PHA800 (pre). Statistical analysis was conducted using the unpaired two-tailed Student's t-test and ANOVA, followed by Tukey's multiple comparison post hoc test. $^{*}p < 0.05$, $^{**}p < 0.01$, $^{***}p < 0.001$, and $^{****}p < 0.0001$.

3. Conclusion

PHA800 upregulates a TLR4 mediated inflammatory response, which is closely associated with calcium influx triggered by the calcium enrichment activity on its surface. PHA1600- and PHA800-pretreatment groups lower the levels of calcium influx and attenuate inflammatory response owing to mild calcium enrichment activity on the surface (Fig. 7).

4. Materials and methods

4.1. PHA preparation

PHA was prepared through chemical and thermal treatments, as previously described [14,15,36]. In brief, cancellous bone obtained from porcine femoral epiphysis was subjected to boiling in distilled water for 2 h to degrease and facilitate the removal of soft tissue such as periosteum and bone marrow. The bones were dissected into regular blocks (5 mm^3) using cut-off machines (Accutom-50, Struers, Ballerup, Denmark) with cooling water. These blocks were then calcinated at 800 °C or 1600 °C, employing a heating rate of 10 °C/min, and maintained at this temperature for 2 h in air within a muffle furnace to obtain PHA800 and PHA1600.

4.2. Physicochemical evaluation

SEM (SU8220, HITACHI, Japan) analysis was performed to observe the surface morphology. The inner morphology was examined using TEM (Tecnai G2 Spirit, FEI, the Netherlands). The elemental composition and distribution were analyzed using EDX (SU8220, HITACHI, Japan). XRD (Empyrean, Panalytical, the Netherlands) was employed for the characterization of crystallization patterns.

4.3. Cell culture

The RAW 264.7 cell line was purchased from Procell Life Science and Technology Co., Ltd. The Dulbecco's modified Eagle's medium (C11885500BT, Thermo Fisher, China) supplemented with 10 % (v/v) fetal bovine serum (10099141, Thermo Fisher, China) and 1 % (v/v) penicillin-streptomycin (15140122 Thermo Fisher, China) was used as a complete culture medium. PHA800 and PHA1600 blocks underwent sterilization via irradiation with gamma rays at a dose of 25 kGy before utilization. Cells were cultured with a complete culture medium under a humidified atmosphere containing 5 % CO_2 at 37 °C, with passages performed at a 1:3 ratio upon achieving 80 % confluence.

For indirect culture with conditioned medium (Strategy 1), the complete medium was added with PHA800 with a ratio of 50 mg/ml for 24 h. After centrifugation at 1000*g* for 5 min, the supernatant was aspirated and filtered using a 0.22 μm filter to obtain the conditioned medium. Cells were then cultured with the conditioned medium for cytotoxicity assay and PCR analysis. For direct co-culture (Strategy 2), cells were cultured with the complete medium with PHA800 in a ratio of 20 mg/ml for RNA extraction. For direct co-culture (Strategy 3), PHA800 was grinding and sieving to obtain particles under 250 μm. Cells were cultured with a complete medium with PHA800 in a ratio of 5/1/0.2/0.04 mg/ml respectively for cytotoxicity assay and PCR analysis. PHA1600 was tested for cytotoxicity and RNA extraction at a concentration of 1 mg/ml.

4.4. Cytotoxicity assay

Cytotoxicity assay was used to screen suitable cell culture models using the CCK-8 cell counting kit (CK04, DOJINDO, Japan). Cells were resuspended and seeded at a density of 2000 cells per well on a 96-well plate, followed by incubation with complete medium, conditioned medium, or direct culture with PHA800 and PHA1600. The medium was renewed every 2 days. At day 1, 3, and 5, the medium was exchanged with DMEM solution containing 10 % CCK-8, and the cells underwent a 1 h incubation period. The absorbance (OD value) of individual wells was measured at 450 nm using a microplate analyzer (Epoch2, America). Five wells were analyzed in parallel for each group.

4.5. RNA-seq and bioinformatic analysis

RNA-seq was used to reveal the main activation pathways of cellular inflammatory response. Total RNA extraction of raw 264.7 was conducted using TRIzol (R0016, Beyotime, China) after 1 day culture. To synthesize cDNA, RNA samples were first purified, fragmented, and

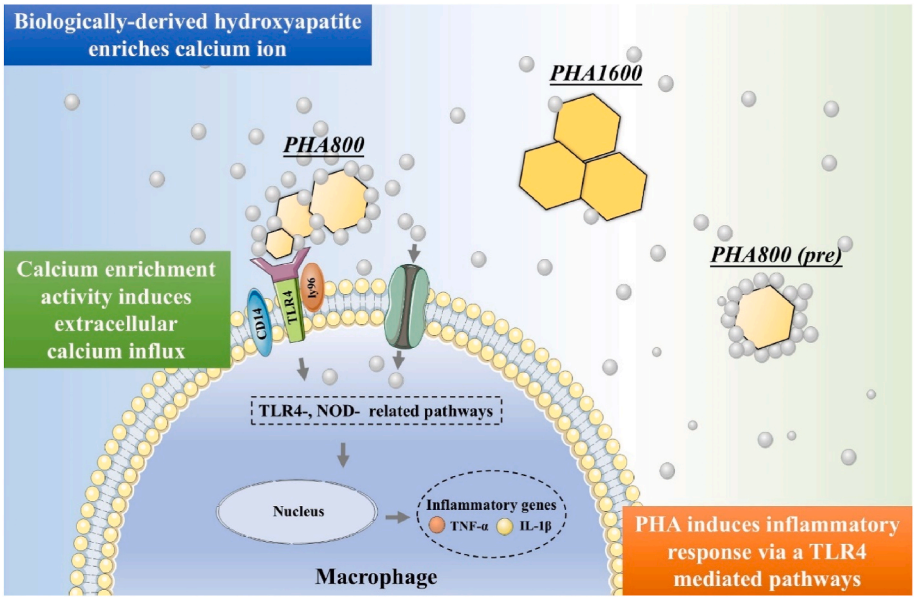

Fig. 7. Schematic figure of porcine bone-derived hydroxyapatite triggering inflammatory response of macrophages. Active calcium enrichment on PHA800 surface initiates calcium influx, leading to the upregulation of a potential TLR4-, NOD-related inflammatory response. The calcium enrichment activity remained low at the surface of PHA1600 and PHA800 (pre), which inhibited the initiation of calcium influx leading to a decreased inflammatory response compared with PHA800.

reverse transcribed into cDNA. BGI Group was responsible for the preparation of the entire cDNA library and the sequencing of the transcriptome. The transcriptome sequencing data generated were subjected to screening using SOAPnuke (version 1.5.2) and then aligned to the reference genome using HISAT2 (version 2.0.4). The position information of the confirmed sequences in the genome was obtained using Bowtie2 (version 2.2.5) with clean reads. The expression levels of genes were calculated using RSEM (version 1.2.8) software. The analysis was conducted using the Dr.Tom platform (https://biosys.bgi.com), which employed two commonly used indicators, TPM and FPKM, to reflect gene abundance. Differential expression analysis was performed using the DESeq2 tool. The criteria for filtering in the analysis were: when the |log2(FC)| value of a gene was greater than 1 and the *Q*-value was less than 0.05, the gene expression difference was considered significant and included in subsequent analysis.

Principal component analysis (PCA), Gene Ontology (GO) analysis of biological processes, cellular components, and molecular function, Kyoto Encyclopedia of Genes and Genome (KEGG) pathway, analysis were conducted using the Dr.Tom platform and DAvID Bioinformatics Resources (v6.8). Cytoscape plugin ClueGO was used (v2.5.8) for further visualization of REACTOME enrichment analysis and gene correlation analysis. Data visualization was performed using TBtools (version 1.100), R Studio (version 5.0), GraphPad Prism (version 9.0.0), and the Hiplot platform (https://hiplot.com.cn/). The bioinformatics analysis and data visualization were completed by the researchers.

4.6. RT-qPCR analysis

RT-qPCR was used to validate transcriptomic results and to assess the level of inflammation at the gene level. Total RNA extraction of raw 264.7 was conducted using TRIzol (R0016, Beyotime, China) after 6 h culture. RNA samples from each group were subjected to concentration and purity detection by measuring absorbance at wavelengths of 280 nm and 260 nm. Following the instructions of the reverse transcription kit, 500 ng of RNA was used for cDNA synthesis using the Synthesis SuperMix kit (11141ES60, YEASEN, China). The Hieff qPCR SYBR Green Master Mix (11202ES08, YEASEN, China) was used to perform RT-qPCR. Subsequently, based on the cDNA sequence information provided by NCBI, corresponding primers were designed and validated using the BLAST database (Supplementary Table 5). GAPDH was chosen as the reference gene, and mRNA expression levels of related genes were detected using SYBR real-time fluorescence quantitative PCR pre-mix in a 384-well plate.

4.7. Enzyme-linked immunosorbent assay (ELISA) detection

TNF-α was selected to validate the transcriptomic results and further evaluate the inflammatory level of pretreated PHA800. After 1/2/3 days' incubation, supernatants were extracted respectively. The protein expression levels of TNF-α were detected using an ELISA kit (CSB-E08054m, CUSABIO, China) following the instructions provided. Briefly, 100 μl supernatants were added to the ELISA plate. The liquid was removed after 2 h incubation. Biotin-antibody (100 μl) was added and removed after 1 h incubation followed by washing. HRP-avidin was added and removed after 1 h incubation followed by washing. TMB substrate was added in the dark at 37 °C for 30 min. Stop solution was added to stop the chromogenic reaction. The OD value was measured at 450 nm using a multifunctional microplate reader (CSB-E04741m-IS, CUSABIO, China). The concentration is calculated according to the standard curve and formula provided in the instructions.

4.8. Intracellular calcium detection

Intracellular calcium detection was used to clarify the role of calcium channels and cytosolic calcium ions in the activation of inflammatory pathways. Fluo-4 AM (S1061S, BEYOTIME, China) was used to measure the cytoplasmic calcium concentration in macrophage cells. After cell adherence, hydroxyapatite suspension (100 μl) was added to each well, and the plates were further incubated at 37 °C for 0.5/6/12/24 h. At each timepoint, the culture medium was aspirated from the wells, and the plates were washed twice with PBS to remove excess hydroxyapatite. Fluo-4 working solution was then prepared according to the instructions and added (100 μl) to each well, incubate at 37 °C in the dark for 30 min. The fluorescence intensity was measured using a fluorescence microplate reader with Ex/Em wavelengths of 490/525 nm (Synergy H1, Biotek, USA). Typical fluorescence images were captured using a fluorescence microscope with Ex/Em wavelengths of 470/525 nm (Axio, Zeiss, Germany).

Calcium channel blocking model: TRPM7 inhibitor FTY720 (10 nM) was added to each well and incubated for 6 h. The medium was removed, following 100 μl hydroxyapatite suspension added to each well for 24 h. Fluo-4 working solution was prepared according to the instructions and added to each well, incubating at 37 °C in the dark for 30 min. The fluorescence intensity was measured using a fluorescence microplate reader (Ex/Em = 490/525 nm).

PHA800 pretreated model: PHA800 was immersed in complete medium at 2 mg/ml for 48 h. The medium was removed by centrifugation at 1000 rpm for 5 min to obtain PHA800 (pre). Samples were prepared for subsequent intracellurlar calcium detection and PCR test.

4.9. Calcium enrichment activity evaluation

Inductively coupled plasma-optical emission spectroscopy (ICP-OES, Agilient 720 ES, USA) was used to describe the calcium enrichment activity on the surface of bone substitute. Firstly, PHA800/1600 was placed in DMEM solution in 10 mg/ml. The concentration of Ca^{2+} in the supernatant was measured using inductively coupled plasma-optical emission spectroscopy (ICP-OES) after 24 h incubation. According to the result, a specific sequential ICP detection of Ca^{2+} in PHA800 was implemented at 5 min/2/6/12/24/48 h of incubation.

4.10. Statistical analysis

Data were expressed as mean ± standard deviation when they followed a normal distribution. Before intergroup comparison, homogeneity of variance was confirmed. Non-paired t-tests were used for comparisons between the two groups. For comparisons among multiple groups with equal variances, one-way analysis of variance (ANOVA) was employed, followed by Tukey's Honestly Significant Difference (HSD) post-hoc test for pairwise comparisons. If the variances were unequal, the Kruskal-Wallis test was used. Statistical analysis was performed using GraphPad Prism (version 9.0.0), with p-values <0.05 considered statistically significant (*$p < 0.05$; **$p < 0.01$; ***$p < 0.001$; ****$p < 0.0001$). The absence of asterisks indicates no statistically significant differences in the data.

CRediT authorship contribution statement

Chuangji Li: Writing – original draft, Methodology, Conceptualization. **Mengxi Su:** Writing – original draft, Methodology, Conceptualization. **Meihua Mai:** Writing – original draft, Methodology, Conceptualization. **Zefeng Guo:** Investigation, Data curation. **Ye Li:** Investigation, Data curation. **Shoucheng Chen:** Visualization. **Quan Liu:** Visualization. **Danying Chen:** Visualization. **Xiayi Wu:** Visualization. **Zetao Chen:** Supervision, Funding acquisition. **Zhuofan Chen:** Supervision, Funding acquisition. **Shiyu Wu:** Writing – review & editing, Supervision, Conceptualization.

Declaration of competing interest

The authors declare that they have no known competing financial interests or personal relationships that could have appeared to influence

the work reported in this paper.

Data availability

The authors do not have permission to share data.

Acknowledgments

This study was supported by the Guangzhou Science and Technology Foundation and Application Foundation Research Topic (2024A04J2458), Open Project of State Key Laboratory of Oral Disease (SKLOD2019OF08) and National Natural Science Foundation of China under grant numbers 81970975, 81901055, 82001095, and 82201095.

Appendix A. Supplementary data

Supplementary data to this article can be found online at https://doi.org/10.1016/j.mtbio.2024.101231.

References

[1] R.A. Scott, ITI treatment guide, volume 5: sinus floor elevation procedures, Br. Dent. J. 212 (10) (2012) 512, 512.
[2] D. Wismeijer, S. Chen, D. Buser, I.T.I. Treatment Guide, 7 Vol, Ridge Augmentation Procedures in Implant Patients: A Staged Approach, vol. 232, Quintessence pub, 2014.
[3] F. Velard, et al., Inflammatory cell response to calcium phosphate biomaterial particles: an overview, Acta Biomater. 9 (2) (2013) 4956–4963.
[4] Y. Harada, et al., Differential effects of different forms of hydroxyapatite and hydroxyapatite/tricalcium phosphate particulates on human monocyte/macrophages in vitro, J. Biomed. Mater. Res. 31 (1) (1996) 19–26.
[5] Z. Chen, et al., Osteoimmunomodulation for the development of advanced bone biomaterials, Mater. Today 19 (6) (2016) 304–321.
[6] P. Luo, et al., Tailoring the multiscale mechanics of tunable decellularized extracellular matrix (dECM) for wound healing through immunomodulation, Bioact. Mater. 28 (2023) 95–111.
[7] R. Liu, et al., Immunomodulation-based strategy for improving soft tissue and metal implant integration and its implications in the development of metal soft tissue materials, Adv. Funct. Mater. 30 (2020) 1910672.
[8] X. Wang, et al., Alteration of clot architecture using bone substitute biomaterials (beta-tricalcium phosphate) significantly delays the early bone healing process, J. Mater. Chem. B 6 (48) (2018) 8204–8213.
[9] P. Lagadec, et al., Calcium supplementation decreases BCP-induced inflammatory processes in blood cells through the NLRP3 inflammasome down-regulation, Acta Biomater. 57 (2017) 462–471.
[10] D. Buser, 30 Years of Guided Bone Regeneration, third ed., Quintessence Publishing Co., Inc., 2022.
[11] S. Bailliez, A. Nzihou, The kinetics of surface area reduction during isothermal sintering of hydroxyapatite adsorbent, Chem. Eng. J. 98 (1) (2004) 141–152.
[12] O. Prokopiev, I. Sevostianov, Dependence of the mechanical properties of sintered hydroxyapatite on the sintering temperature, Mater. Sci. Eng., A 431 (1) (2006) 218–227.
[13] A. Grandjean-Laquerriere, et al., Involvement of toll-like receptor 4 in the inflammatory reaction induced by hydroxyapatite particles, Biomaterials 28 (3) (2007) 400–404.
[14] W. Qiao, et al., Changes in physicochemical and biological properties of porcine bone derived hydroxyapatite induced by the incorporation of fluoride, Sci. Technol. Adv. Mater. 18 (1) (2017) 110–121.
[15] R. Liu, et al., Fluorination enhances the osteogenic capacity of porcine hydroxyapatite, Tissue Eng. 24 (15–16) (2018) 1207–1217.
[16] Y. Liu, et al., Effects of fluorinated porcine hydroxyapatite on lateral ridge augmentation: an experimental study in the canine mandible, Am J Transl Res 12 (6) (2020) 2473–2487.
[17] Q. Liu, et al., Preparation and characterization of fluorinated porcine hydroxyapatite, Dent. Mater. J. 31 (5) (2012) 742–750.
[18] S. Mondal, et al., Hydroxyapatite: a journey from biomaterials to advanced functional materials, Adv. Colloid Interface Sci. 321 (2023) 103013.
[19] J.M. Sadowska, J. Guillem-Marti, M.P. Ginebra, The influence of physicochemical properties of biomimetic hydroxyapatite on the in vitro behavior of endothelial progenitor cells and their interaction with mesenchymal stem cells, Adv. Healthcare Mater. 8 (2) (2019) e1801138.
[20] Y. Hua, et al., Exposure to hydroxyapatite nanoparticles enhances Toll-like receptor 4 signal transduction and overcomes endotoxin tolerance in vitro and in vivo, Acta Biomater. 135 (2021) 650–662.
[21] R. Wang, et al., Hydroxyapatite nanoparticles promote TLR4 agonist-mediated anti-tumor immunity through synergically enhanced macrophage polarization, Acta Biomater. 164 (2023) 626–640.
[22] J.M. Sadowska, et al., Effect of nano-structural properties of biomimetic hydroxyapatite on osteoimmunomodulation, Biomaterials 181 (2018) 318–332.
[23] Y. Hua, et al., Exposure to hydroxyapatite nanoparticles enhances Toll-like receptor 4 signal transduction and overcomes endotoxin tolerance in vitro and in vivo, Acta Biomater. 135 (2021) 650–662.
[24] W. Strober, et al., Signalling pathways and molecular interactions of NOD1 and NOD2, Nat. Rev. Immunol. 6 (1) (2006) 9–20.
[25] M.S. Schappe, et al., Chanzyme TRPM7 mediates the Ca(2+) influx essential for lipopolysaccharide-induced toll-like receptor 4 endocytosis and macrophage activation, Immunity 48 (1) (2018) 59–74.e5.
[26] Ž. Mladenović, et al., In vitro study of the biological interface of Bio-Oss: implications of the experimental setup, Clin. Oral Implants Res. 24 (3) (2013) 329–335.
[27] H.M. Kim, et al., Process and kinetics of bonelike apatite formation on sintered hydroxyapatite in a simulated body fluid, Biomaterials 26 (21) (2005) 4366–4373.
[28] S.S. Jensen, et al., Tissue reaction and material characteristics of four bone substitutes, Int. J. Oral Maxillofac. Implants 11 (1) (1996) 55–66.
[29] M. Thorwarth, et al., Evaluation of substitutes for bone: comparison of microradiographic and histological assessments, Br. J. Oral Maxillofac. Surg. 45 (1) (2007) 41–47.
[30] J.C. Taylor, et al., In vitro osteoclast resorption of bone substitute biomaterials used for implant site augmentation: a pilot study, Int. J. Oral Maxillofac. Implants 17 (3) (2002) 321–330.
[31] J.L. Ong, et al., Osteoblast precursor cell activity on HA surfaces of different treatments, J. Biomed. Mater. Res. 39 (2) (1998) 176–183.
[32] G. Liu, et al., Modulating the cobalt dose range to manipulate multisystem cooperation in bone environment: a strategy to resolve the controversies about cobalt use for orthopedic applications, Theranostics 10 (3) (2020) 1074–1089.
[33] S. Wu, et al., Sodium fluoride under dose range of 2.4-24 μM, a promising osteoimmunomodulatory agent for vascularized bone formation, ACS Biomater. Sci. Eng. 5 (2) (2019) 817–830.
[34] Y. Wu, et al., Optimizing the bio-degradability and biocompatibility of a biogenic collagen membrane through cross-linking and zinc-doped hydroxyapatite, Acta Biomater. 143 (2022) 159–172.
[35] Y. Xing, et al., Optimized osteogenesis of porcine bone-derived xenograft through surface coating of magnesium-doped nanohydroxyapatite, Biomed. Mater. 18 (5) (2023).
[36] Z. Li, et al., Effects of fluoridation of porcine hydroxyapatite on osteoblastic activity of human MG63 cells, Sci. Technol. Adv. Mater. 16 (3) (2015) 035006.